Proceedings of Symposium on Ultrasonic Electronics, Vol. 35 (2014) pp. 17-18
3-5 December, 2014

Mechanoluminescent materials and their applications
応力発光材料の開発と応用

Chao-Nan XU[1,2,3†]
([1]National Institute of Adv. Indust. Sci. and Tech. (AIST), [2]Interdisciplinary Grad. School Eng. Sci., Kyushu Univ, [3]International Institute for Carbon Neutral Energy Research (WPI-I^{2}CNER), Kyushu Univ.)
徐　超男 [1,2,3†]　([1](独)産総研　九州, [2]九州大学大院　総合理工,　[3]九州大学　WPI-I^{2}CNER)

Recently, we developed innovative elasticoluminescent (ESL) materials, each particle of which repeatedly emits visible light in response to stress. Distinct from other kinds of mechanoliminescence (ML), the ESL is reproducible by mechanical stimulation. When a structure is coated with such a material, each particle acts as a sensitive mechanical sensor, and the two-dimensional emission pattern of the entire assembly represents an accurate reflection of the dynamical strain (stress) distribution of the structure.[1-6)]

This novel approach enables diagnostics of structural health, with a number of advantages over the conventional point-by-point measurement method using a strain gauge. With the proposed technique, defects invisible with the naked eye and microscopic cracks in small parts of machinery can be detected, and the safety of largescale constructions such as bridges can be monitored with respect to various types of vibration and damage. In this manner, the use of the proposed ESL technology is expected to pave the way for novel methods for structural health diagnosis.[7-18)]

We have confirmed that the ESL intensity distribution is in excellent agreement with the distribution of equivalent stress and the distribution of strain/deformation energy, which are related to damage, even under complex conditions. Also, a comparison between the measured stress values and the safety standard values can aid the process of elucidating the level of danger imposed by defects.

By covering the entire target area under observation, measurements and inspections based on ESL can reveal localized cracks emerging in this area and can provide a high-resolution representation of the corresponding strain/stress distribution and danger level.

This is one of the main characteristics of ESL-based technology, which is expected to provide the basis of not only new methods for stress analysis, but also an entire new industry centered on the inspection of structural safety.

Here, we show the example of visualization of ultrasonic power distribution. The ultrasonic power

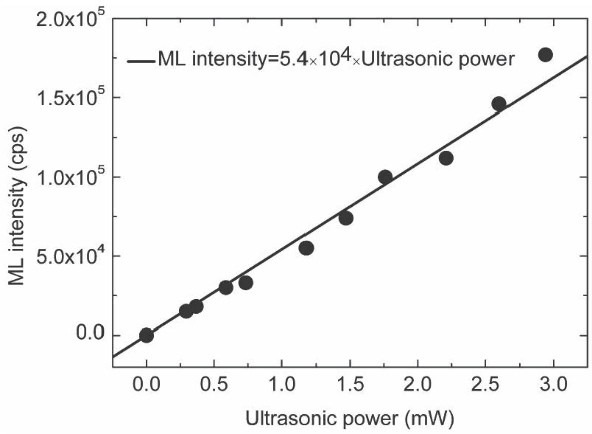

Fig. 1 Relationship between ML intensity and ultrasonic output power.

is not distributed uniformly over the area of an ultrasonic pulse. Therefore, with respect to potential biological effects of the ultrasonic wave including thermal effect and cavitations, it is not sufficient to measure only the total output power of the transducer so that, the measurement of ultrasonic output power distribution is also of great significance. However, it has been difficult to do such measurements by conventional methods. In this study, two transducers with different frequency and shape were used to produce ultrasonic vibration; a CCD camera was used to record ML images during the application of ultrasonic vibration to the ML film. A luminescent region on the ML sensing film was observed during the application of ultrasonic vibration, the shape and size of the region was the same as that of the piezoelectric ceramic patch of the transducer, as shown in **Fig. 2(a) and (b)**. The distribution of ML intensity along the X-axis is plotted in **Fig. 2(c)**. In order to visualize the distribution of ultrasonic power density, a calibration curve between the grayscale value of the image and the power density was constructed according to the relationship shown in **Fig. 1**.

Figure 3. shows the three-dimensional representation of the ultrasonic output power distribution. As shown in this figure, the distribution of ultrasonic output power was near a normal distribution; the power density in the central area was the largest. By comparison the output power of the transducer with 6 MHz was only about one fifth of that of the transducer with 20 MHz.

----

e-mail:cn-xu@aist.go.jp

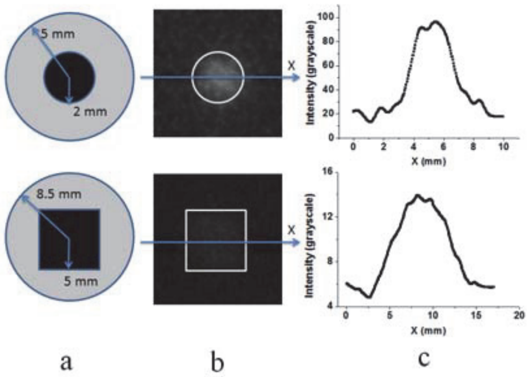

Fig 2. (a) Cross-sectional view of the transducers (Outer: epoxy resin; central: piezoelectric ceramic patch). (b) ML images recorded during ultrasonic vibration. (c) Distribution of ML intensity along X-axis. (Up: 20 MHz; below: 6 MHz)

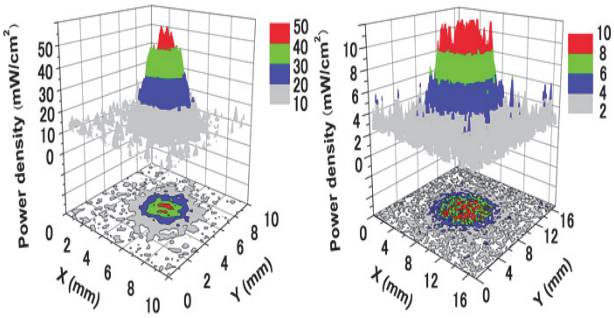

Fig 3. Three-dimensional representation of ultrasonic output power distribution of two transducers. (Left: 20 MHz; right: 6 MHz)

approach, the ultrasonic output power distribution of the transducer could be visualized simply and directly by measuring the ML distribution.

Acknowledgment

The research presented in this paper is the result of collaborative research conducted by a large number of collaborators. We express our gratitude specially to Ueno N, Imai Y, Terasaki N, Yamada H, Adachi Y, Nishikubo K, Fukuda O, Bu N, Ono D, Li C, Zhang L, Hyodo K, Guo S, Zhan T, and all member of Advanced Integrated Sensing Team from AIST, Zheng X, and others from Saga University, Prof. Wang W and others from Kyushu University, Takemura T from Nihon University, Tsuji T and others from Logical Products, Inc., Shinokawa T and others from Taisei Kisosekkei Co., Ltd,, and Kawabata Y, Iwanami M, and others from the Port and Airport Research Institute. This research was funded in part under the CREST program established by JST. We are deeply indebted to the Land Management Office in Asakura, Fukuoka Prefecture, Koutou-ku, Tokyo, Osaka, respectively, for kindly permitting the use of the bridges for the experiments presented in this paper.

References

1. C. N. Xu: Ceramics. **44** (2009) 154.
2. C. N. Xu: Oyo Buturi. **80** (2011) 46.
3. C. N. Xu: Encycl. Smart Mater. **1** (2006) 190.
4. C. N. Xu, H. Yamada, X. S. Wang and X. G. Zheng: Appl. Phys. Lett. **84**(2004) 3040.
5. C. N. Xu, T. Watanabe, M. Akiyama and X. G. Zheng: Appl. Phys. Lett. **74**(1999) 2414.
6. Advanced Industrial Science and Technology (AIST), Advanced Integrated Sensing Team home page, 2001-2014, see: https://unit.aist.go.jp/msrc/ja/teams/03_advanced .html
7. N. Ueno, D. Ono and C.N. Xu: T. SICE 2011. 47.
8. C. Li, C. N. Xu, L. Zhang, H. Yamada and Y. Imai: J. Visualization. **11**(2008) 329.
9. C. S. Li, C. N. Xu, Y. Imai, W. X. Wang, L. Zhang and H. Yamada: Appl. Mech. Mater. **13-14**(2008) 247.
10. K. Hyodo, C. N. Xu, H. Mishima and S. Miyakawa: Proc. IFMBE. **31**(2010) 545.
11. Y. Terasawa, C. N. Xu and K. Hyodo: Proc. JSEM 2011.
12. Y. Imai, C. N. Xu and W.X. Wang: Proc. 4th Int. Symp. on Advan. Fluid/Solid Sci. and Tech. in Exp. Mech. 2009, MA-III-4.
13. R. J. Sanford: *Principles of Fracture Mechanics* (Upper Saddle River, NJ, 2003).
14. C. S. Li, C. N. Xu, Y. Imai and N. Bu: Strain. 2012.
15. D. Ono, C. Z. Li, N. Bu and C. N. Xu: J. JSEM **10**(2010) 152.
16. D. Ono, Y. Kawabata, C. S. Li, C. Z. Li, N. Ueno, M. Iwanami and C. N. Xu: J. Visualization Soc. Jpn. **30**(2010) 343.
17. Y. Kawabata, D. Ono, C. Li, E. Kawasaki, M. Iwanami, E. Kato, N. Ueno and C. N. Xu: J. JSCE **67**(2011) 430.
18. C. N. Xu: Cem. Concr. **764**(2010) 8.
19. T.Z. Zhan, C.N. Xu*, O. Fukuda, H. Yamada and C.S. Li: Ultrasonics Sonochemistry, **18**(2011) 436.
20. T.Z. Zhan, C.N. Xu*, O. Fukuda, H. Yamada, C.S. Li: IOP Conference Series: Materials Science and Engineering. **18**(2011) 212011